Journal of Research and Applications in Mechanical Engineering
ISSN: 2229-2152 (Print); 2697-424x (Online)
(2025) Vol. 13, No. 1, Paper No. JRAME-25-13-013
[DOI: 10.14456/jrame.2025.13]

Research Article

Parametric Optimization for Dimensional Accuracy and Surface Roughness in Additive Manufactured Novel Acetabular Liner using Two Different Techniques

J. Sofia
N. Ethiraj*
Department of Mechanical Engineering, Dr.M.G..R Educational and Research Institute, Maduravoyal, Chennai-600095, India

Received 3 July 2024
Revised 18 September 2024
Accepted 20 September 2024

Abstract:
Fused Filament Fabrication (FFF), also known as Fused Deposition Modeling (FDM), is a widely utilized additive manufacturing technique. By fine-tuning process parameters, improvements in product quality can be achieved. This study investigates optimizing parameters: print speed, layer height, and infill density in fabricating acetabular liners, a component of hip implants using FFF. Four decision-making methods namely the Analytic Hierarchy Process (AHP) combined with Technique for Order of Preference by Similarity to Ideal Solution (AHP-TOPSIS), Entropy Weight Method (EWM)-TOPSIS, AHP-Multi-Objective Optimization on the basis of Ratio Analysis (MOORA), and EWM-MOORA) are compared to identify the most suitable parameter settings. Observations from Experiments are used in each method. The research evaluates these methods to determine the optimal FFF parameters and the results will help to improve the 3D Printing process through informed parameter selection.

Keywords: *Additive manufacturing, Fused filament fabrication, Optimization, TOPSIS, MOORA, AHP*

1. Introduction

Additive manufacturing (AM) or 3D printing is a cutting-edge technique for producing goods by layering computer models into actual items. In contrast to conventional manufacturing technologies, which generally entail removing material from a solid block, additive manufacturing involves gradually adding material to create the finished object. This technology is transforming many industries, including consumer products, automotive, aerospace, and healthcare, by making it possible to create complex designs with increased precision and customization [1]. AM finds extensive application in various medical domains, including medication delivery, in-vitro technologies, and 4D printing. The pharmaceutical business uses AM in several ways, including Screw Extrusion Additive Manufacturing and Stereolithography for diagnostic procedures. External prostheses are also made using Fused Filament Fabrication (FFF), Selective Laser Sintering (SLS), and Melt Electrospinning Writing (MEW) [2]. Fused Filament Fabrication is a popular manufacturing concept employed by companies and researchers due to its low cost, short turnaround time, and high accuracy. Replacement of human tissues, bones, and joints is just one of the numerous biomedical applications for which Fused Deposition Modelling (FDM) is an excellent method [3].

* Corresponding author: N.Ethiraj
E-mail address: ethiraj.mech@drmgrdu.ac.in

The Total Hip Arthroplasty (THA), sometimes referred to as Total Hip Replacement, is a sophisticated surgical procedure used to substitute damaged or broken hip components with prosthetic implants. A vital component of the total hip arthroplasty prosthesis is the acetabular liner. It is positioned precisely inside the acetabular cup. The liner is an extra layer between the acetabular cup and the femoral head, acting as a protective cushion [4, 5]. It was successfully fabricated using FFF as the process has evolved from making prototypes to final product production. Optimizing the 3D printing process is necessary to ensure mass-produced items meet high standards pertaining to mechanical and quality aspects for enhanced performance. In recent years, considerable studies have been undertaken for optimizing numerous process variables, such as extruder temperature, raster angle, layer thickness, raster gap, raster width, contour width, and specimen orientation, to produce the best required mechanical properties possible. Achieving optimal process parameters in manufacturing often necessitates balancing multiple, sometimes conflicting, objectives. To address this challenge, researchers have adopted a diverse array of optimization techniques, including Taguchi-based Simple Additive Weighting (SAW), VIekriterijumsko KOmpromisno Rangiranje (VIKOR), Technique for Order of Preference by Similarity to Ideal Solution (TOPSIS), Electre technique, Grey Relational Analysis (GRA), and Particle Swarm Optimization (PSO). These methods have demonstrably yielded success in optimizing turning parameters for tool life and surface roughness [6], welding parameters for mechanical properties [7], friction stir welding parameters [8], and electrochemical machining process parameters for dimensional accuracy and material removal rate [9]. The selection of the most suitable optimization technique is paramount for ensuring the achievement of desired outcomes across a wide spectrum of manufacturing processes.

The Analytic Hierarchy Process (AHP), developed in the 1970s, aids in complex decision-making by breaking down problems into hierarchical criteria and alternatives. Through pairwise comparisons, AHP quantifies both qualitative and quantitative factors, facilitating informed evaluations. Its versatility has led to widespread adoption across various fields. Rakhade et al. [10] used AHP and TOPSIS to select 3D printers, while Al Theeb et al. [11] applied AHP and combined AHP-TOPSIS to identify optimal waste-to-energy technology for Jordan. Ccatamayo-Barrios et al. [12] used AHP and TOPSIS for mining method selection in Peru's Gol Gohar mine. The Entropy Weight Method (EWM) has become a prominent model in decision-making, gaining attention in academia and practical applications. Its key advantage lies in reducing human bias compared to subjective methods, by objectively assigning weights to criteria based on information content in the decision matrix. This data-driven approach enhances objectivity and reliability, leading to widespread adoption across decision-making domains. Li et al. [13] applied EWM to evaluate coal mine safety, demonstrating its reliability with TOPSIS. Zhao et al. [14] integrated EWM and TOPSIS for sustainable island development, validated in a case study of Dachan Island. Zhang [15] used EWM and TOPSIS for power grid supplier evaluation, offering a dependable selection framework. Zhu et al. [16] explored EWM in water source site selection, highlighting potential distortions with Monte Carlo Simulation.

Multi-Objective Optimization by Ratio Analysis (MOORA) is a decision-making technique that selects the optimal alternative from a group of possibilities based on a variety of factors. Each criterion is given a weight, and alternatives are ranked depending on their performance about these weights. MOORA seeks to discover the best solution that maximizes benefits while minimizing expenses across different objectives. Sahu et al. [17] compared the performance of AlSiMg electrodes manufactured using the SLS technique to that of conventional copper and brass electrodes. The MOORA method was used to optimize parameters for achieving a better surface finish in the EDM process and optimal parameters were found to be discharge current = 10A and pulse-on-time =100µs, and AlSiMg RP tool electrode. Paul and Das [18] explored the use of Fuzzy Analytic Hierarchy Process and MOORA for optimizing layer height, print speed, and orientation minimizing printing time and printing cost. It was found that layer thickness increases, print times are reduced and print speeds improve as well. Print time is significantly impacted by the construction orientation. Shihab et al. [19] applied MOORA method to identify the parameters voltage, torch angle, and current to reduce both the power and duration of the cladding process. Syed et al. [20] utilized the Grey-Taguchi methodology to enhance FDM parameters for optimizing tensile strength, flexural strength, and longitudinal shrinkage. They identify key parameters like layer thickness, raster angle, fill density, contours, printing temperature, and speed, optimizing them to minimize shrinkage while maximizing strengths. Yang et al. [21] focused on maximizing tensile strength and minimizing surface roughness and build time in FDM through central composite design, leveraging response surface methodology combined with genetic algorithms. Ganapathy et al. [22] predicted surface finish and delamination factor in FDM using machine learning models, emphasizing process parameters like printing temperature, layer height, raster angle, and fill pattern. Kónya [23] determined optimal layer thickness and component orientation for improved surface roughness and accuracy, favoring vertical orientation.

Fountas et al. [24] studied nozzle temperature and layer thickness effects on surface roughness in FDM, achieving minimum roughness with specific parameter settings. Mohanty et al. [25] investigated the impact of processing constraints on dimensional accuracy, employing Taguchi's methodology and various optimization techniques. Begovic et al. [26] optimized gear torque using Taguchi method, identifying optimal values for factors like wall thickness and infill, enhancing torque performance. Tura and Mamo [27] employed hybrid methodologies to improve flexural strength in FDM, emphasizing the influence of raster angle. Shirmohammadi et al. [28] optimized surface roughness using neural networks and particle swarm algorithms, achieving superior results with specific parameter settings. Hasdiansah et al. [29] reported surface roughness optimization in Thermoplastic Polyurethane (TPU) 3D printing via Taguchi approach, identifying optimal process parameters. Tuncel [30] analyzed the impact of layer height, infill density, and print speed on the compressive strength of ABS samples using Taguchi design and ANOVA. Chohan et al. [31] employed TOPSIS for the optimization of tensile strength, surface roughness, and weights of ABS samples made by FDM. In summary, the review reveals that while various combination optimization techniques have been employed for multi-parameter optimization, there is relatively less exploration in the integration of different weighting methods with an optimization technique. This research focuses on utilizing two techniques of weight evaluation in combination with TOPSIS and MOORA for optimizing dimensional accuracy and surface roughness of acetabular liners made by FFF process.

2. Experimental Setup

The acetabular liners were fabricated using two filament materials, polylactic acid (PLA) and high-impact polystyrene (HIPS). Material selection was based on biocompatibility and desired degradation profile. PLA offers biocompatibility and biodegradability, ideal for applications requiring implant degradation. Conversely, HIPS possessed biocompatibility but lacked biodegradability. Both filaments (1.75mm diameter) were acquired from World of Lilliput (WOL) 3D. The proposed liner design employed a PLA core of thickness 8 mm encapsulated within HIPS layers of thickness 2mm for degradation protection. Additionally, the top layer utilized HIPS to shield PLA from bodily fluids. The important dimensions of the designed liner are shown in Fig. 1. A Divide by Zero Model 250 printer with dual nozzles facilitated the fabrication of acetabular liners which is presented in Fig. 2. Three printing parameters such as slice height, infill density, and print speed were used for investigations, with different levels provided in Table 1. Taguchi's L9 Orthogonal array served as the experimental design, enabling the exploration of various parameter combinations across multiple levels which is presented in Table 2. The subsequent section outlines the nine experiments conducted for sample fabrication.

Table 1: Control parameters and their levels

Parameter/Level	Level 1	Level 2	Level 3
Print Speed in mm/sec	30	40	50
Layer Height in mm	0.1	0.2	0.3
Infill Density in %	40	60	80

Table 2: L_9 inner orthogonal array

Experiment No	Print Speed	Layer Height	Infill density
1	30	0.1	40
2	30	0.2	60
3	30	0.3	80
4	40	0.1	60
5	40	0.2	80
6	40	0.3	40
7	50	0.1	80
8	50	0.2	40
9	50	0.3	60

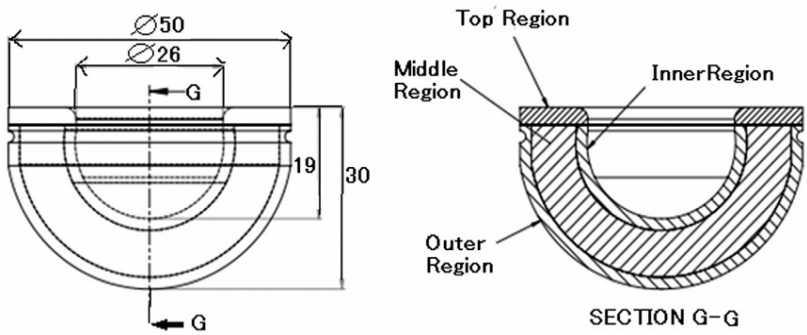

Fig. 1. Important dimensions of the designed acetabular liner

Fig. 2. Used 3D printer

The fabrication of designed dual materials acetabular liner in the 3D printer (Fig. 3) is shown. Support material is used during fabrication and these materials are removed once the process is completed. The dimensional accuracy and surface quality of the fabricated acetabular liners were evaluated. Dimensional measurements, including height (H), inner diameter (ID), and external diameter (ED), were performed using a coordinate measuring machine (CMM) (Zeiss Contura G2, MPE_E = (1.8 + L/300μm), MPE_P = 1.8μm). The CMM is equipped with a ZEISS VAST XT scanning probe and CALYPSO 4.8 measurement software. Surface profile roughness (Ra) was measured using a Mitutoyo SJ-410 surface roughness tester with a least count of 0.01μm.

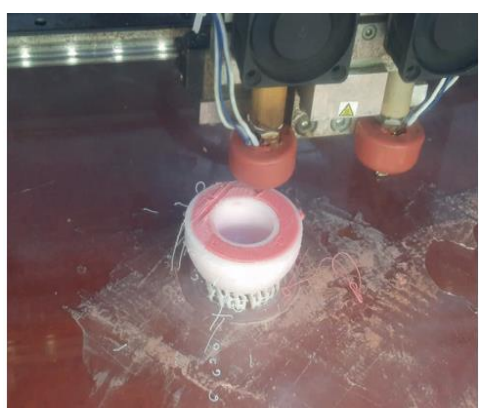

Fig. 3. Acetabular liners fabricated by FFF

3. Data Processing

3.1 Analytic Hierarchy Process

Thomas Saaty developed the Analytic Hierarchy Process (AHP) in 1980 as a method to decompose and analyze complex problems hierarchically [14]. The scale for the relative importance of the parameters is displayed in Table 3.

Table 3: Scale of relative importance

	Importance	**Meaning of attributes**
1	Equal importance	Two attributes are equally important
3	Moderate importance	One attribute is moderately important over the other
5	Strong importance	One attribute is strongly important over the other
7	Very importance	One attribute is very important over the other
9	Absolute importance	One attribute is absolutely important over the other
2,4,6,8	Compromise importance between 1,3,5 and 9	

The matrix A is constructed based on pairwise comparisons, with each element Aij representing the comparison between the i^{th} row and the j^{th} column. The pairwise comparisons are illustrated in Table 4. The value 1 implies equal relevance, while the value 7 shows that the EH is seven times as essential as the SR. As a result, the SR is 1/7 times more essential than the EH

Table 4: Pairwise Comparison of desired parameters

	Surface Roughness SR	**Error in Height EH**	**Error in ED EED**	**Error in ID EID**
SR	1	7	5	3
EH	1/7	1	1/3	1/5
EED	1/5	3	1	1/3
EID	1/3	5	3	1

$$GM_i = \left\{ \prod_{j=1}^{b} a_{ij} \right\}^{1/b} \tag{1}$$

$$W_j = {GM_i}\Big/{\sum_{i=1}^{N} GM_i} \tag{2}$$

Where a_{ij} is the element in i^{th} row and j_{th} column of matrix A.

To ensure consistent comparison among the responses listed in Table 4, the following procedure is applied:
Initially, the weighted sum of the responses and their corresponding eigenvalues (λ) for each row is calculated using Formula (3).

$$\lambda_i = {\sum_{j=1}^{b} W_j X_{ij}}\Big/{W_i} \tag{3}$$

Next, the maximum eigenvalue (λ_{max}) using Equation (4) is determined.

$$\lambda_{max} = {\sum_{i=1}^{a} \lambda_i}\Big/{a} \tag{4}$$

As per Satty (1977), a Consistency Index (CI) is computed using Formula (5).

$$CI = {(\lambda_{max} - n)}\Big/{(n-1)} \tag{5}$$

The resulting CI value is then compared with the relevant Random Consistency Index (RI) obtained from Table 5.

Table 5: Random Consistency Index (RI)

N	**3**	**4**	**5**	**6**	**7**	**8**	**9**	**10**
RI	0.58	0.90	1.12	1.24	1.32	1.41	1.45	1.49

Finally, the Consistency Ratio (CR) is calculated using the equation (6)

$$CR = {CI}/{RI} \tag{6}$$

If the computed CR value falls below 10% (0.1), indicating a consistent and acceptable pairwise comparison matrix (A), the results are considered reliable. However, when the CR value exceeds 10%, adjustments to the pairwise comparison values are necessary to ensure consistency and reliability.

3.2 Entropy

The first step is the standardization of measured values. The standardized value of the measure in the i th row and j th column is denoted by P_{ij} and is calculated as:

$$P_{ij} = {x_{ij}}/{\sum_{j=1}^{n} x_{ij}} \tag{7}$$

In the Entropy method, the entropy value E_{ij} is defined by

$$E_i = -{\sum_{j=1}^{n} P_{ij} * \log_n P_{ij}}/{\log_n n} \tag{8}$$

Weights are calculated based on the entropy values

$$W_i = {(1 - E_i)}/{\sum_{i=1}^{m}(1 - E_i)} \tag{9}$$

3.3 TOPSIS Optimization

In the TOPSIS technique, each criterion progresses in either a continuously increasing or decreasing order. As a result, it provides a solution that is not only closest to the theoretically best but also farthest from the theoretically worst option [10].

Step 1: Compute the normalized performance ratings.

In this process, every performance rating xij within X is divided by its respective norm. This yields the normalized ratings yij (where i = 1,2, …I; j = 1,2,…J) which can then be computed using the below Eq.(10).

$$y_{ij} = {x_{ij}}/{\sqrt{\sum_{i=1}^{I} x_{ij}^2}} \tag{10}$$

This conversion method makes it easier to compare attributes by using dimensionless units. However, because the scale lengths are not identical, it makes direct comparisons difficult. The normalised performance ratings yij can be given as a matrix Y as shown in Eq. (11).

$$Y = \begin{bmatrix} y_{11} & y_{12} & \cdots & y_{1J} \\ y_{21} & y_{22} & \cdots & y_{2J} \\ \cdots & \cdots & \cdots & \cdots \\ y_{I1} & y_{I2} & \cdots & y_{IJ} \end{bmatrix} \tag{11}$$

Step 2: The weights obtained from AHP or Entropy methods are combined with the ratings.

The weighted and normalised performance rating (i =1,2,…, I;j=1,2,…,J) is calculated as shown in Eq. (12). These weighted ratings are combined to form the weighted-normalized decision matrix V in Eq. (13).

$$\upsilon_{ij} = W_j * y_{ij};\ (i=1,2,\ldots,I;\ j=1,2,\ldots..J) \tag{12}$$

$$V = \begin{bmatrix} \upsilon_{11} & \upsilon_{12} & \ldots & \upsilon_{1J} \\ \upsilon_{21} & \upsilon_{22} & \ldots & \upsilon_{2J} \\ \ldots & \ldots & \ldots & \ldots \\ \upsilon_{I1} & \upsilon_{I2} & \ldots & \upsilon_{IJ} \end{bmatrix} \tag{13}$$

Step 3: Determine the positive and negative ideal solutions.

A^* and $A^-$are denoted as the positive and negative ideal solution sets respectively which can be detected from Eq. (13) as

$$A^* = \left[\upsilon_1^*, \upsilon_2^*, \ldots\ldots, \upsilon_J^*\right] \tag{14}$$

$$A^- = \left[\upsilon_1^-, \upsilon_2^-, \ldots\ldots, \upsilon_J^-\right] \tag{15}$$

where,

$$v_j^* = \begin{Bmatrix} \max v_{ij}, \text{if j is a benefit attribute} \\ \max v_{ij}, \text{if j is a cost attribute} \end{Bmatrix}$$

$$v_j^- = \begin{Bmatrix} \min v_{ij}, \text{if j is a benefit attribute} \\ \min v_{ij}, \text{if j is a cost attribute} \end{Bmatrix}$$

Step 4: Derive the separation values

The separation measure is the distance of each alternative rating from both the positive and negative ideal solutions which is obtained by applying the Euclidean distance theory. Eqs. (16) & (17) show the process for positive and negative separation calculations respectively.

$$S_i^+ = \sqrt{\sum_{j=1}^{J}(\upsilon_{ij} - \upsilon_j)^2} \tag{16}$$

$$S_i^- = \sqrt{\sum_{j=1}^{J}(\upsilon_{ij} - \upsilon_j^-)^2} \tag{17}$$

Step 5: Calculate the overall preference score

The overall preference score υ_i for each alternative A_i is obtained as shown in Eq. (18).

$$\upsilon_i = {S_i^-}\Big/{S_i^- + S_i^+} \tag{18}$$

Alternatives are ranked based on higher υ_i values.

3.4 MOORA Optimization

The methodology of the MOORA method is outlined as follows:

1. Compute the normalized value.

$$X_{ij} = {}^{X_{ij}}\Big/\sqrt{\sum_{i=1}^{m} X_{ij}^2} \tag{19}$$

Where Xij = observed responses of the i^{th} number of experiments in the j^{th} response, m is the number of experiments and n is the number of responses.

X^*_{ij} = normalized value of the i^{th} number of experiments in the jth response. It is a dimensionless number, which lies between 0 and 1.

2. Determine the normalized assessment value.

$$y_i = \sum_{j=1}^{g} W_j X_{ij}^* - \sum_{j=g+1}^{n} W_j X_{ij}^* \tag{20}$$

Where g = normalized number of responses,
n-g = minimized number of responses,
W_j = weight of the j^{th} response.

In maximization problems, the normalized value is added, while in minimization problems, it is subtracted.

4. Results and Discussion

The acetabular liners are manufactured using FFF and the output responses namely surface roughness, error in height, error in external diameter, and Error in internal diameter are found and tabulated as shown in Table 6.

Table 6: Response values

Expt. No	SR	EH	EED	EID
1	11.78	0.05	0.1	0.15
2	11.4	0.13	0.17	0.35
3	12.69	0.08	0.19	0.81
4	11.7	0.05	0.32	1.82
5	12.38	0.08	0.32	0.29
6	11.72	0.37	0.27	0.36
7	10.88	0.15	0.14	1.87
8	11.89	0.22	0.25	0.32
9	11.92	0.17	0.25	0.14

The research is done in four stages:

- First, the Calculation of Weights using AHP, and an alternative method for AHP, Entropy
- Using the weights obtained from AHP and Entropy, TOPSIS approach is applied for optimization.
- The Third stage comprises finding optimal process parameters by adopting MOORA method,
- Fourthly, a Comparison of the methods is performed.

4.1 Determination of Weights

4.1.1 Weight Computation using AHP

The geometrical mean, weights and their corresponding eigen values are calculated using the equations 1-4 and displayed in Table 7.

Table 7: Weights and consistency index

Responses	SR	EH	EED	EID	GM	W	λ
SR	1.00	7	5	3	3.20	0.56	4.12
EH	0.14	1	0.33	0.20	0.31	0.06	4.13
EED	0.20	3	1	0.33	0.67	0.12	4.10
EID	0.33	5	3	1	1.49	0.26	4.10
$\lambda max = Mean\ of\ \lambda$							**4.117**
Consistency Index = 0.03898 Consistency Ratio = 0.04331							

The consistency index and Consistency ratio are calculated using the equations 5 & 6 and are shown in Table 7 to check the consistency of the pairwise comparison. With a CR of less than 0.1, the weightage and, consequently the pairwise comparisons are considered reliable and acceptable.

4.1.2 Weight Computation using ENTROPY Method

From the responses in Table 6, the standardised values are calculated using equation 7. The corresponding entropy value and the weights are determined using the equation 8 and 9 and presented in Table 8.

Table 8: Entropy and weights

Expt. No	Standardised Value			
	SR	EH	EED	EID
1	0.111	0.025	0.050	0.025
2	0.107	0.031	0.085	0.059
3	0.119	0.016	0.095	0.144
4	0.110	0.008	0.159	0.379
5	0.116	0.010	0.159	0.097
6	0.110	0.042	0.134	0.012
7	0.102	0.016	0.070	0.062
8	0.112	0.023	0.124	0.011
9	0.112	0.018	0.124	0.005
E_i	4.826	1.561	4.702	3.147
W_i	0.374	0.055	0.362	0.210

4.2 TOPSIS Optimization

4.2.1 AHP - TOPSIS

For performing optimization, the response values have to be normalised, therefore the outcomes are normalised using the Eq. (10) and expressed as matrix N according to equation (11).

$$N = \begin{pmatrix} 0.332 & 0.096 & 0.142 & 0.053 \\ 0.321 & 0.250 & 0.241 & 0.124 \\ 0.358 & 0.154 & 0.269 & 0.287 \\ 0.330 & 0.096 & 0.454 & 0.646 \\ 0.349 & 0.154 & 0.454 & 0.103 \\ 0.330 & 0.710 & 0.383 & 0.128 \\ 0.307 & 0.288 & 0.199 & 0.663 \\ 0.335 & 0.422 & 0.355 & 0.114 \\ 0.336 & 0.326 & 0.355 & 0.050 \end{pmatrix}$$

The rank of the experiments is given based on the RCR values. The RCR values in turn are dependent on the ideal solutions computed. The normalized performance matrix and rank computations were used to evaluate the effectiveness of different options in a decision-making process. Each alternative was evaluated using criteria such as SR, EH, EED, and EID, and the accompanying scores indicated its performance. The weighted normalized values,

S^+ and S^- values were then calculated using the Eqs. (12) – (18) to determine how close each alternative is to the ideal and negative ideal solutions, respectively and presented in Table 9 along with the ranking.

4.2.2 Entropy TOPSIS

The normalised performance matrix N of the outcomes already determined is used for the weighted performance matrix and rank calculations. The weighted performance matrix is shown in Table 10, where the performance of each option is multiplied by its assigned weight. Experiment 1 is the best option, closely followed by experiment 2 based on the computed S^+ and S^- values. Regarding appropriateness, experiment 9 and 8 stands in third and fourth rank respectively.

4.3 MOORA Optimization

4.3.1 MOORA with AHP

First, the weighted matrix is calculated using weights from AHP and the normalized values N. The second step is to find the normalized assessment values utilizing equation 20 which is presented in Table 11.

Table 9: Calculations of Weighted performance, Rank by AHP -TOPSIS

SR	EH	EED	EID	S^+	S^-	RCR	Rank
0.187	0.005	0.017	0.014	0.016	0.169	0.914	1
0.181	0.014	0.028	0.033	0.023	0.148	0.863	2
0.202	0.008	0.032	0.076	0.069	0.106	0.604	7
0.186	0.005	0.054	0.170	0.160	0.038	0.190	9
0.197	0.008	0.054	0.027	0.041	0.151	0.786	5
0.186	0.039	0.045	0.034	0.047	0.142	0.751	6
0.173	0.016	0.023	0.174	0.162	0.048	0.228	8
0.189	0.023	0.042	0.030	0.035	0.147	0.809	4
0.189	0.018	0.042	0.013	0.028	0.164	0.855	3

Table 10: Weighted performance matrix, Rank Calculations by Entropy - TOPSIS

SR	EH	EED	EID	S^+	S^-	RCR	RANK
0.124	0.005	0.051	0.011	0.023	0.174	0.885	1
0.120	0.014	0.087	0.026	0.024	0.140	0.853	2
0.134	0.008	0.098	0.060	0.059	0.108	0.645	5
0.123	0.005	0.164	0.136	0.156	0.036	0.186	9
0.130	0.008	0.164	0.022	0.094	0.122	0.563	7
0.124	0.039	0.139	0.027	0.077	0.116	0.600	6
0.115	0.016	0.072	0.139	0.129	0.097	0.429	8
0.125	0.023	0.128	0.024	0.062	0.122	0.665	4
0.126	0.018	0.128	0.010	0.059	0.136	0.697	3

Table 11: Calculated Weights and Ranking by AHP – MOORA

Weighted Standard Decision Matrix				Contribution Index	RANK
SR	EH	EED	EID		
0.186	0.006	0.017	0.014	-0.223	1
0.180	0.015	0.029	0.032	-0.256	2
0.200	0.009	0.032	0.075	-0.317	7
0.185	0.006	0.054	0.168	-0.413	9
0.195	0.009	0.054	0.027	-0.286	5
0.185	0.043	0.046	0.033	-0.307	6
0.172	0.017	0.024	0.172	-0.385	8
0.188	0.025	0.043	0.030	-0.285	4
0.188	0.020	0.043	0.013	-0.263	3

4.3.2 MOORA with Entropy

Similarly, the normalized assessment values are calculated by incorporating weights from entropy and are shown in Table 12. In MOORA with AHP, experiment 1 has the largest weighted score and hence the highest contribution Index, making it the top-ranked option. Experiment 2 is close behind in second place. Similarly, in MOORA with Entropy, experiment 1 maintains its lead with the greatest Contribution Index and experiment 2 again takes second place.

Table 12: Calculated Weights and Ranking by Entropy – MOORA

Weighted Standard Decision Matrix				Contribution Index	RANK
SR	EH	EED	EID		
0.124	0.005	0.051	0.011	-0.192	1
0.120	0.014	0.087	0.026	-0.247	2
0.134	0.008	0.098	0.060	-0.300	4
0.123	0.005	0.164	0.136	-0.428	9
0.130	0.008	0.164	0.022	-0.325	6
0.124	0.039	0.139	0.027	-0.328	7
0.115	0.016	0.072	0.139	-0.342	8
0.125	0.023	0.128	0.024	-0.301	5
0.126	0.018	0.128	0.010	-0.282	3

4.4 Comparison of TOPSIS and MOORA

Table 13 shows the ranks derived from four distinct approaches: MOORA with AHP, MOORA with Entropy, AHP TOPSIS, and Entropy TOPSIS, for each experiment. Experiments 1,2,4,7 and 9 have consistent rankings across all four methodologies. Experiments 6 and 8 show uniformity with all three methods except for MOORA with Entropy. It is observed from the research that the AHP when used with both the optimization techniques yields similar results, whereas the entropy weight method shows little difference in the middle rankings. The optimal process parameters from the different optimization approaches affecting the surface roughness, height, external diameter, and internal diameter of the acetabular liner are found to be a print speed of 30 mm/sec, layer height of 0.1, and infill density of 40%. This is analogous to the results obtained by Hasdiansah et al. [29] incorporating the Taguchi method, and Morvayová et al. [32] using Grey Relational Analysis in combination with Taguchi.

Table 13: Comparison of Ranks obtained from four approaches

Experiment No.	MOORA AHP	MOORA ENTROPY	AHP TOPSIS	ENTROPY TOPSIS
1	1	1	1	1
2	2	2	2	2
3	7	4	7	5
4	9	9	9	9
5	5	6	5	7
6	6	7	6	6
7	8	8	8	8
8	4	5	4	4
9	3	3	3	3

The reason for the best result may be attributed to the following: (i) At lower layer height the materials flow smoothly and help to reduce the staircase effect; (ii) Since the print speed is less, the layers have enough time to cool and when the next layer is added it gels with the printed layer allowing better dimensional accuracy; (iii) The effect of compressive force of the newly formed layer on the already deposited layer is less for the infill density of 40% which prevents the flow of material inside the inner diameter of the liner. This has resulted in better dimensional accuracy. Experiment 4 exhibits the lowest rank due to the higher print speed and infill density. At high print speed, before the printed layer cools completely the next layer is added. Also at high infill density the material in the top layer compresses the deposited layer and therefore it starts flowing from the printed area on either side. The support material prevents flow outside and hence the material flows towards the inner diameter. This has resulted in poor dimensional accuracy of the inner diameter. The samples exhibiting first rank and last rank are shown the Fig. 4(a) and (b).

(a) (b)

Fig. 4. Liner fabricated with (a) print speed 30 mm/sec, Layer height 0.1 mm, and Infill density 40%;(b) print speed 40 mm/sec, Layer height 0.1 mm, and Infill density 60%

5. Conclusion

The FFF process was used to fabricate acetabular liners and tested for surface roughness and dimensional accuracy. The AHP and Entropy were used for calculating the weights of the relative importance of the factors. Further, TOPSIS and MOORA optimization techniques were used to identify the optimal parameters. The following conclusions were drawn:

- AHP, when combined with both MOORA and TOPSIS, produces similar results.
- The Entropy method shows slight variations in middle rankings.
- Optimal process parameters yield the lower surface roughness, reduced error in height, external diameter, and internal diameter of the acetabular liner are at print speed of 30 mm/sec; layer height of 0.1; and fill density of 40% within the experimented process parameters.
- The process parameters print speed 40 mm/sec, layer height 0.1 mm, and infill density 60% yielded the lowest rank with both MOORA and TOPSIS.
- Further consideration of different machines, other process parameters and external conditions may yield a different optimal solution.

Acknowledgment

We sincerely thank the management of Dr. M.G.R. Educational and Research Institute for their continuous support and encouragement.

References

[1] Gade S, Vagge S, Rathod M. A review on additive manufacturing – methods, materials, and its associated failures. Adv Sci Technol Res J. 2023;17(3):40-63.

[2] Monfared V, Ramakrishna S, Nasajpour-Esfahani N, Toghraie D, Hekmatifar M, Rahmati S. Science and technology of additive manufacturing progress: processes, materials, and applications. Met Mater Int. 2023;29(12):3442-3470.

[3] Montez M, Willis K, Rendler H, Marshall C, Rubio E, Rajak DK, et al. Fused deposition modeling (FDM): processes, material properties, and applications. In: Kumar P, Misra M, Menezes PL, editors. Tribology and Surface Engineering, Tribology of Additively Manufactured Materials. Amsterdam: Elsevier, 2022. p. 137-163.

[4] Sofia J, Ethiraj N, Nikolova MP. Preliminary study on the additively manufactured plastic liner of an acetabular cup component. Jurnal Teknologi. 2022;84(2):113-120.

[5] Sofia J, Ethiraj N, Nikolova MP. A novel method of fabricating multi-material acetabular liner using fused filament fabrication. Polym Eng Sci. 2023;63(12):4140-4152.

[6] Ingle S, Raut D. Evaluation of tool wears mechanism considering machining parameters and performance parameters for titanium alloy in turning operation on CNC. Adv Mater Process Technol. 2024;10(3):1380-1400.
[7] Koli Y, Yuvaraj N, Aravindan S, Vipin. Multi-Response mathematical model for optimization of process parameters in CMT welding of dissimilar thickness AA6061-T6 and AA6082-T6 alloys Using RSM-GRA coupled with PCA. Adv Ind Manuf Eng. 2021;2:100050.
[8] Meikeerthy S, Ethiraj N. Multi response optimization of friction stir welding in air and water by analytic hierarchy process and VIKOR method. Scientia Iranica. 2024;31(4):346-357.
[9] Rao PV, Pawar PJ, Shankar R. Multi-objective optimization of electrochemical machining process parameters using a particle swarm optimization algorithm. Proc Inst Mech Eng Part B: J Eng Manuf. 2008;222(8):949-958.
[10] Rakhade RD, Patil NV, Pardeshi MR, Patil BG. Selection of 3D printer for innovation centre of academic institution based on AHP and TOPSIS methods. Int J Res Appl Sci Eng Technol. 2021;9(12):1872-1880.
[11] Al Theeb N, Abu Qdais H, Abu Qdais FH, Habibah O. Utilizing AHP-TOPSIS as multi-criteria decision approaches to select the best alternative for waste to energy technology. Jordan J Mech Ind Eng. 2022;16(4):601-613.
[12] Ccatamayo-Barrios JH, Huamán-Romaní YL, Seminario-Morales MV, Flores-Castillo MM, Gutiérrez-Gómez E, Carrillo-De la cruz LK, et al. Comparative analysis of AHP and TOPSIS multi-criteria decision-making methods for mining method selection. Math Model Eng Probl. 2023;10(5):1665-1674.
[13] Li X, Wang K, Liu L, Xin J, Yang H, Gao C. Application of the entropy weight and TOPSIS method in safety evaluation of coal mines. Procedia Eng. 2011;26:2085-2091.
[14] Zhao DY, Ma YY, Lin HL. Using the entropy and TOPSIS models to evaluate sustainable development of islands: a case in china. Sustainability. 2022;14(6):3707.
[15] Zhang Y. TOPSIS method based on entropy weight for supplier evaluation of power grid enterprise. Proceedings of the 2015 International Conference on Education Reform and Modern Management; 2015 Apr 19-20; Hong Kong. Amsterdam: Atlantis Press; 2015. p. 334-337.
[16] Zhu Y, Tian D, Yan F. Effectiveness of entropy weight method in decision-making. Math Probl Eng. 2020;2020:1-5.
[17] Sahu AK, Mahapatra SS, Chatterjee S, Thomas J. Optimization of surface roughness by MOORA method in EDM by electrode prepared via selective laser sintering process. Mater Today: Proc. 2018;5(9):19019-19026.
[18] Paul A, Das MC. A decision support system for the selection of FDM process parameters using MOORA. Manag Sci Lett. 2024;14:181-188.
[19] Shihab SK, Khan NZ, Myla P, Upadhyay S, Khan ZA, Siddiquee AN. Application of MOORA method for multi optimization of GMAW process parameters in stain-less steel cladding. Manag Sci Lett. 2018;8:241-246.
[20] Syed MAB, Rahman Q, Shahriar HM, Khan MMA. Grey Taguchi approach to optimize Fused Deposition Modeling process in terms of mechanical properties and dimensional accuracy. J Eng Res Innov Educ. 2022;4(1):38-52.
[21] Yang L, Li S, Li Y, Yang M, Yuan Q. Experimental investigations for optimizing the extrusion parameters on FDM PLA printed parts. J Mater Eng Perform. 2019;28(1):169-182.
[22] Ganapathy SB, Sakthivel AR, Kandasamy J, Khan T, Aloufi M. Optimization of printing process variables and the effect of post-heat treatments on the mechanical properties of extruded polylactic acid–aluminum composites. Polymers. 2023;15(24):4698.
[23] Kónya G. Investigating the impact of productivity on surface roughness and dimensional accuracy in FDM 3D printing. Period Polytech Transp Eng. 2024;52(2):128-133.
[24] Fountas N, Kechagias J, Vaxevanidis N. Statistical modeling and optimization of surface roughness for PLA and PLA/wood FDM fabricated items. J Mater Eng. 2023;1(1):38-44.
[25] Mohanty A, Nag KS, Bagal DK, Barua A, Jeet S, Mahapatra SS, et al. Parametric optimization of parameters affecting dimension precision of FDM printed part using hybrid taguchi-MARCOS-nature inspired heuristic optimization technique. Mater Today: Proc. 2022;50:893-903.
[26] Begovic E, Plancic I, Ekinovic S, Sarajlic A. FDM 3D printing process parameters optimization using taguchi method for improving the gear strength. Int J Adv Res. 2022;10(3):782-788.
[27] Tura AD, Mamo HB. Characterization and parametric optimization of additive manufacturing process for enhancing mechanical properties. Heliyon. 2022;8(7):e09832.

[28] Shirmohammadi M, Goushchi SJ, Keshtiban PM. Optimization of 3D printing process parameters to minimize surface roughness with hybrid artificial neural network model and particle swarm algorithm. Prog Addit Manuf. 2021;6(2):199-215.
[29] Hasdiansah H, Yaqin RI, Pristiansyah P, Umar ML, Priyambodo BH. FDM-3D printing parameter optimization using taguchi approach on surface roughness of thermoplastic polyurethane parts. Int J Interact Des Manuf. 2023;17(6):3011-3024.
[30] Tuncel O. Optimization of specific compression strength of abs samples produced with FDM by taguchi method. The 5th International Conference of Materials and Engineering Technology; 2023 Nov 13-16; Trabzon, Turkey. p. 120-129.
[31] Chohan JS, Kumar R, Singh TB, Singh S, Sharma S, Singh J, et al. Taguchi S/N and TOPSIS based optimization of fused deposition modelling and vapor finishing process for manufacturing of ABS plastic parts. Materials. 2020;13(22):5176.
[32] Morvayová A, Contuzzi N, Fabbiano L, Casalino G. Multi-attribute decision making: parametric optimization and modeling of the FDM manufacturing process using PLA/wood biocomposites. Materials. 2024;17(4):924.